Submitted to "Nuclear Physics" UM-P-82/59.

Variations of the Gyromagnetic Ratios of Low-Lying States in ^{192}Os

H.H. Bolotin, I. Morrison, C.G. Ryan

School of Physics, University of Melbourne, Parkville, Victoria 3052, Australia

and

A.E. Stuchbery

School of Physics, University of Melbourne, Parkville, Victoria 3052, Australia

and

Department of Nuclear Physics, Research School of Physical Sciences,
Australian National University, Canberra, A.C.T. 2600, Australia

Abstract: The gyromagnetic ratios of the 2_2^+ and 4_1^+ states in ^{192}Os were measured relative to that of its 2_1^+ level. The thin-foil, perturbed γ-ray angular distribution technique was employed utilizing the enhanced transient hyperfine magnetic field present at the nuclei of these ions as they swiftly recoiled through a thin, magnetized Co foil. The states of interest were Coulomb excited using a beam of 220-MeV ^{58}Ni ions. The present measurements yielded ratios $g(2_2^+)/g(2_1^+) = 0.68 \pm 0.08$ and $g(4_1^+)/g(2_1^+) = 1.00 \pm 0.12$. The sizable disparity in the measured g-factors of the levels of the two low-lying bands is compared with interacting boson approximation model-based calculations, as well as with a Nilsson basis single-particle model description.

[NUCLEAR REACTIONS $^{192}Os(^{58}Ni,^{58}Ni'\gamma)$ $^{192}Os(2_1^+,2_2^+,4_1^+)$, E = 220 MeV; measured $\gamma(\theta,H,T)$ in polarized Co, particle-γ coin, Coulomb excitation. ^{192}Os levels deduced g. Enriched target, thin foil technique.
NUCLEAR STRUCTURE $^{190,192}Os$; calculated g. Interacting boson approximation, broken O(6) symmetry; Nilsson basis single-particle model.]

1. Introduction.

In recent papers,[1-3] both our experimental measurements and interacting boson approximation (IBA) (Ref.4-6) model-based calculations of the absolute and relative B(E2) transition rates between levels in ^{196,198}Pt and the gyromagnetic ratios of the 2_1^+, 2_2^+, and 4_1^+ levels in these nuclides were reported. In these, it was demonstrated that in the near-O(6) (Ref.7) limiting IBA symmetry, with the inclusion of a relatively small symmetry-breaking $\underline{Q}\cdot\underline{Q}$ force and using the same parameters of the interactions that had been shown[1] to account well for both the measured B(E2) rates and $Q(2_1^+)$ values of the even $^{194-198}$Pt isotopes, the gyromagnetic ratios of these levels were predicted to depart from constancy to a small extent. Although the experimental g-factors obtained for these levels in ^{196,198}Pt (Refs.2 and 3) were not inconsistent with these predicted small departures from equality, comparisons with the measured g-factors did not prove as definitive as might otherwise be desired.

In as much as a number of salient nuclear structure aspects of the "transitional" Os and Pt nuclides have not been adequately or self-consistently encompassed by any specific theoretical model description and remain of long-standing interest, we have undertaken, as foreshadowed earlier,[2,3] both experimentally and theoretically to extend these studies to the low-lying excited states in the even Os isotopes where a larger degree of symmetry-breaking departure from the pure O(6)-limit IBA is expected[8] to pertain than for the Pt nuclides. To this end, we present

here our experimental determinations of the gyromagnetic ratios of the 2_1^+, 2_2^+, and 4_1^+ excited states in ^{192}Os and compare these results with IBA-based theoretical predictions, as well as with corresponding alternative calculations in the projected Hartree-Fock formalism using deformed single-particle orbitals.

2. Experimental procedure.

The states of interest in ^{192}Os were Coulomb excited by 220-MeV ^{58}Ni ions from the Australian National University 14 UD Pelletron tandem accelerator. Two HP Ge detectors placed 5 cm from the target at $\pm 65^\circ$ to the incident beam direction registered the de-excitation γ-ray transitions in coincidence with beam projectiles backscattered from the target in the angular range 146°-166° and detected in a common annular surface-barrier detector. The coincidence restriction resulted in events recorded for ^{192}Os ions that recoiled in a forward cone of mean half-angle $\sim 7^\circ$ with a mean initial velocity $v/c = 0.039$. The target (specifically designed for an experimental study[9] of the relative transient hyperfine field strengths acting on Os and Pt ions recoiling through thin, magnetized Co foils) consisted of a lead-backed 4.2 μm Co foil on the up-stream side of which was an electroplated layer of ^{192}Os [(938 ± 66) μg cm^{-2} enriched to 99.06%] on which a (361 ± 25) μg cm^{-2} thick layer of ^{198}Pt (enriched to 95.83%) was electrodeposited. The thicknesses of the Os and Pt layers and of the Co foil were determined by Rutherford scattering of 3-MeV proton from the University of Melbourne 5U Pelletron accelerator and from the yields of detected characteristic X-ray induced by the same proton beam; these results were in accord with the observed Coulomb excitation yields of the ^{192}Os and ^{198}Pt de-excitation γ-rays.

The thin foil, layered target technique employed in the present transient field precession measurements has been described in detail elsewhere[2,10,11]. A polarizing field of 850 Oe was applied to the target; its direction normal to the beam axis was reversed at frequent intervals to minimize systematic errors. Effective magnetic shielding of the fringing field rendered beam-bending effects small compared with the measured precessions (and associated errors) of all states of interest in the present study.

The unperturbed angular distributions of all de-excitation γ rays were measured with the same detectors and geometrical arrangement used in the precession studies. Any local, angularly-dependent γ-ray absorption variations due to non-uniformities in the target chamber walls, etc., were determined and corrected for by measurement, as a function of angle, of the detected rates of γ rays from a ^{152}Eu source placed at the beam spot location behind the target.

For a given γ-ray angular distribution $W(\theta)$, it can readily be shown that the counting rate N recorded by a gamma-ray detector at a specified distance from the target is most sensitive to the transient field-induced angular precession, $\Delta\theta$, of that distribution when located at that angle θ_γ to the beam such that S^2N is a maximum. [S is the logarithmic derivative of $W(\theta)$.] For the target-to-detector distance of

the HP Ge detectors employed in the present investigations, θ_γ was close to $\pm 65^\circ$ for all E2 transitions studied; consequently, the two γ-ray detectors were positioned at these angles to the beam direction.

Coincidences between each γ-ray detector and the projectiles backscattered from the target were recorded in an event-by-event, multiparameter mode on magnetic tape (γ-ray, particle, and time-analog converted pulse-heights, together with a field-up/field-down tag bit). The coincidence spectrum associated with each γ-ray detector and each field direction was obtained separately in off-line tape play-back sorts. Chance coincidence rates, although quite small throughout the experiment, were duly subtracted in the analysis.

3. Analysis of data and other experimental features.

The measured unperturbed γ-ray angular distributions for all transitions observed were in accord with those calculated for the same detectors and detector placements using the Winther-de Boer[12] Coulomb excitation code with feeding from higher states directly populated in the reaction taken into account.

For the case, as is the situation in the present study, where the mean lives of all relevant states are long compared

with the transit time of ions through the polarized ferromagnetic foil, only when an excited state is directly populated in the reaction will it undergo a precession in the transient hyperfine field; that precession will be reflected in a given finite rotation of the angular distribution not only of the γ ray de-exciting that level, but of the angular distributions of all subsequent cascade transitions involved in the specific de-excitation decay pathway to the ground state. Thus, the measured angular distribution of a given transition de-exciting a particular excited state of interest which can be both directly and indirectly populated in the reaction will display a resultant angular displacement that is a weighted average of the precessions in the transient field of that level and those of directly populated higher states which feed it. These weights involve the g-factors of all such states, the strengths of direct population of these higher states relative to that of the state of interest, and the appropriate successive products of the de-excitation transition branching ratios of all levels involved in the various decay pathways leading to indirect population of the specific lower state under consideration.

Therefore, the ratio, ρ, of the normalized counting rate of a specific $J \rightarrow J'$ transition for polarizing field up ($N\uparrow$) to that with field down ($N\downarrow$) registered in a given γ-ray detector set at θ_γ to the beam direction can be expressed[13] as:

$$\rho = \frac{N\uparrow}{N\downarrow} = \frac{1-g_J R\phi}{1+g_J R\phi}\ , \qquad (1)$$

where

$\phi \equiv (\Delta\theta/g_J) = -(\mu_N/\hbar)\int_0^T B_{TF}\,dt$, T is the transit time of the ions through the ferromagnetic foil, μ_N the nuclear magneton, $\Delta\theta$ the precessional shift of the angular distribution of the $J \rightarrow J'$ γ ray de-exciting the state of interest, B_{TF} represents the velocity-dependent transient field, and

$$R = \frac{\left.\frac{dW(\theta)_{JJ'}}{d\theta}\right|_{\theta_\gamma} + \sum_{I,p}\left(\frac{g_I}{g_J}\right)\eta_{IJ}\prod_I^p\left[b^p(I,I-1)\right]\left.\frac{dW(\theta)^p_{IJ}}{d\theta}\right|_{\theta_\gamma}}{\langle W_{fed}(\theta_\gamma)\rangle\left\{1 + \sum_{I,p}\eta_{IJ}\prod_I^p\left[b^p(I,I-1)\right]\right\}}\ ; \qquad (2)$$

g_J is the g-factor of the state of interest, g_I that of any given higher directly populated state I that decays to the state J by cascade pathway p, η_{IJ} is the ratio of direct population of state I to that of state J, $b^p(I,I-1)$ is the transition branching ratio of each state I leading to the next lower state I-1 in any given decay pathway p leading to state J, $W(\theta)_{JJ'}$ is the unperturbed angular distribution of the $J \rightarrow J'$ transition when the state J is directly populated in the reaction, $W(\theta)^p_{IJ}$ is the unperturbed angular distribution of the $J \rightarrow J'$ transition which results when the level J is populated only by feeding from the decay of the directly populated level I via a specific pathway p, and $\langle W_{fed}(\theta_\gamma)\rangle$ is the weighted average angular distribution, evaluated at θ_γ, of the $J \rightarrow J'$ transition which results by virtue of direct population of state J and all cascade pathway feedings to it from all higher states directly populated. $\langle W_{fed}(\theta_\gamma)\rangle$ is given by

$$\langle W_{fed}(\theta_\gamma)\rangle = \frac{W(\theta)_{JJ'}\Big|_{\theta_\gamma} + \sum_{I,p}\left\{\eta_{IJ}W(\theta)^p_{IJ}\prod_I\left[b^p(I,I-1)\right]\right\}\Big|_{\theta_\gamma}}{1 + \sum_{I,p}\left\{\eta_{IJ}\prod_I\left[b^p(I,I-1)\right]\right\}}; \qquad (3)$$

the sums and products are taken over all populated states, I, of higher excitation energy that decay via the various pathways, p, to the state J of interest.

[For the special case in which the g-factors of all levels directly populated have the common value g, R reduces to

$$R = \frac{1}{\langle W_{fed}(\theta_\gamma)\rangle}\left[\frac{d\langle W_{fed}(\theta)\rangle}{d\theta}\right]\Big|_{\theta_\gamma} = S\Big|_{\theta_\gamma}, \qquad (4)$$

i.e., the logarithmic derivative of $\langle W_{fed}(\theta)\rangle$ evaluated at θ_γ. Under these circumstances, eq.(1) becomes

$$\rho = \frac{N\uparrow}{N\downarrow} = \frac{1-g_J S\phi}{1+g_J S\phi} \qquad (5)$$

The value of $S|_{\theta_\gamma}$ for each transition may be calculated[12,14] for the given experimental geometry, or obtained directly from the measured angular distribution in that geometry of the $J \to J'$ transition.]

In general, when it is not known <u>a priori</u> whether the g-factors of all states (or even a subset of them) are identical, eqs.(4) and (5) are not strictly applicable, and eqs.(1)-(3) must be employed. Such was the case in the

present investigation, and analysis proceeded as follows: the precessional data of the $2_2^+ \rightarrow 0_1^+$ and $4_1^+ \rightarrow 2_1^+$ transitions were first considered separately, as the 4_1^+ level does not feed the 2_2^+ state and these levels were the two highest states for which direct population was sufficiently strong for statistically significant precessional data to be obtained in the present work. As states higher in excitation energy than these were directly populated only relatively weakly, it was found in the analysis of both these states that all summed terms in eqs.(2) and (3) were negligible compared to the leading terms of these expressions even under the extreme assumption that the g-factors of all such higher populated levels were more than twice those of the 2_2^+ and 4_1^+ states. (Thus, in these cases, eqs.(4) and (5) also yield these same results.)

The situation was different, however, for the 2_1^+ level; both the 2_2^+ and 4_1^+ states feed the first excited state and were directly populated with strengths comparable to that of the direct population of the 2_1^+ state. Indeed, indirect feeding from the 2_2^+ and 4_1^+ states to the 2_1^+ level accounted for ~20% and ~49%, respectively, of the total population of the first excited state. Thus, the analysis of the precessional data for the $2_1^+ \rightarrow 0_1^+$ transition necessitated utilization of the previously analyzed results for the 2_2^+ and 4_1^+ levels, the details of the well established level scheme, the measured relative direct populations of all levels, and $W(\theta)_{JJ'}$ and $W(\theta)^p_{IJ}$ (and their derivatives) calculated[12,14] for the detectors and detector-target geometry employed, and evaluated at θ_γ. Aside from the terms in eqs.(2) and (3) which relate to the directly populated 2_2^+ and 4_1^+ states, all

other terms were negligibly small compared to the leading terms in these expressions (again, even under the tenuous assumption that the g-factors of all other states were more than twice that of the 2_1^+ level). [A small correction (0.7 mrad) to the extracted transient field precession of the 2_1^+ state was made for the precession of this long-lived level (τ = 418 psec)[15] in the applied polarizing magnetic field whilst the Os ions resided in the Pb target backing prior to decay. This correction was quite small compared to the measured transient field precession of this level (see below).]

All states higher in excitation than that of the 4_1^+ level were populated too weakly in this study to allow statistically meaningful g-factors to be extracted from the recorded data.

As the mean lives[15] of all states populated in ^{192}Os were long compared to the transit time ($\sim$0.5 psec) of the Os ions through the polarized Co foil employed, corrections for decays in flight while in Co were negligible. The transit time was calculated from the known kinematics and the measured target and Co foil thicknesses using the stopping powers of Ziegler[16].

It should be noted that as the calculated and measured unperturbed angular distributions of the $2_1^+ \rightarrow 0_1^+$ transition were in excellent accord, the Pb target backing proved an effective perturbation-free environment for the 2_1^+ state over the extended period of its long lifetime, save for the small precession of this level in the applied polarizing field.

4. Experimental results.

The relevant portion of the coincidence γ-ray spectrum recorded at 65° to the incident beam direction is presented in fig. 1. [The presence in this spectrum of transitions in ^{195}Pt is due to the nature of the target composition (used in our ancillary study[9]); the Pt transitions do not obscure any of the relevant transitions in ^{192}Os.] The particulars of the experimental precession measurements, their analyzed results, and the g-factors extracted from the analysis presented in Sec. 5 for the 2_1^+, 2_2^+, and 4_1^+ levels in ^{192}Os, are given in table 1. In these results, the g-factor of the 2_1^+ level in ^{192}Os was taken as known [$g(2_1^+;^{192}\text{Os}) = 0.365 \pm 0.010$] from the weighted average of all previously reported[17] determinations of it, and the gyromagnetic ratios of the 2_2^+ and 4_1^+ states were determined relative to it. Thus, that value of $g(2_1^+;^{192}\text{Os})$ served in the analysis to specify the time-integrated transient field also acting on these two higher states (independent of the degree of polarization of the ferromagnetic foil), since the ^{192}Os ions in all three excited states traversed the same polarized Co foil with the same velocity and experienced the same integrated transient field during the same ion transit time τ_{Co} through the foil. This procedure by which the g-factors of all levels are inferred relative to that of a known state renders it unnecessary to rely upon any form of ion velocity- and Z-dependent transient field parameterization - a reliance which has been shown[9] to be questionable in some cases.

The present results for the g-factors in ^{192}Os and those empirically determined by prior authors (where available) for the corresponding levels in the even $^{186-190}$Os isotopes are presented in table 2.

It is clear from the extracted g-factors of the three levels in ^{192}Os that the gyromagnetic ratios of the 2_1^+ and 4_1^+ states are the same, while, in contradistinction, that of the 2_2^+ level differs from them substantially. [Although the single prior measurement[17] of $g(2_2^+)$ reported (see table 1) might have suggested a possible disparity between the g-factors of the 2_1^+ and 2_2^+ states, its relatively large experimental uncertainty could equally well have led to the conclusion that the gyromagnetic ratios of these levels are consistent with being the same. On the other hand, the precision of the present measurements yields a ratio $g(2_2^+)/g(2_1^+)$ that differs substantially from unity by approximately four standard deviations.]

5. Theoretical calculations.

5.1 Gyromagnetic ratios

In view of experimental findings (table 2) that the gyromagnetic ratios in the Os nuclides display (i) relatively large variations for levels in a given isotope and (ii) sizable changes for given corresponding levels in the even Os isotopes as a function of mass, it is of interest to calculate theoretically the g-factors of states in the even Os nuclei - particularly for the (2_1^+, 2_2^+, and 4_1^+) triplet of states in ^{190,192}Os.

Despite the abundance of data, principally in the form of B(E2) transition rates, which supports interpretation of the Os isotopes as rigid triaxial rotors or γ-soft vibrators,[18] the disparities experimentally observed for the g-factors in these nuclides cannot readily be accounted for in terms of shape (β,γ) variations as they are independent of β,γ, and level-spin J to lowest order.[19]

In previous papers,[2,3] we presented a parameterization of g-factor variations in the semi-phenomenological IBA model.[4-7] To recapitulate, the gyromagnetic ratios are given by $g(L) = \mu_L/L$, where

$$\mu_L = \frac{L}{\sqrt{L(L+1)(2L+1)}} \langle L||T(M1)||L\rangle \qquad (6)$$

and T(M1) is the magnetic dipole operator. In the IBA, T is parameterized[2] to second order as

$$T(M1) = g\sqrt{10}\,(d^{\dagger}\tilde{d})^{1}_{\mu} + g_c[(d^{\dagger}s)^{2}\otimes(\tilde{d}^{\dagger}\tilde{d})^{1} + (d^{\dagger}\tilde{d})^{1}\otimes(s^{\dagger}\tilde{d})^{2}]^{1}_{\mu} \qquad (7)$$

where "g" is the level-independent gyromagnetic ratio and g_c is the level-dependent correction (variation). Calculation of boson structure factors together with an experimental measurement of an M1 transition rate enable g_c to be obtained and, hence, the level dependence of g(L) to be evaluated.

The Pt-Os region has been shown to be an interesting and appropriate one for boson models[1,8] both as a detailed test of

symmetry-breaking on B(E2) selection rules and as an exhibition of a phase transition from γ-soft vibrator [O(6) limit] to rotor [SU(3)]. The variations of g-factors will now be discussed in terms of this model.

5.2 IBA-based g-factor calculations

The spectra of ^{190,192}Os were calculated by fitting the parameters (A,B,C,D) of the boson Hamiltonian[1,7]

$$H_B = AP_6 + BC_5 + C\underline{Q}\cdot\underline{Q} + D\underline{L}\cdot\underline{L} \qquad (8)$$

to the low-lying energy levels in a least-squares procedure. The four parameters were free to vary and the solution found is similar to that of Casten et al.[8] [i.e., O(6) + some SU(3) symmetry breaking ($\underline{Q}\cdot\underline{Q} + \underline{L}\cdot\underline{L}$)]; these results are presented in table 3.

The E2 matrix elements can be evaluated by writing the E2 operator to lowest order[6] as

$$T(E2) = \alpha[(s^\dagger d)^2 + (d^\dagger s)^2]^2_\mu + \beta[d^\dagger d]^2_\mu \ ; \qquad (9)$$

and with $(\alpha,\beta) = (16.1, 1.5)$, the calculated quadrupole dynamic and static moments are compared with experimental values in table 4 for the first two excited 2^+ states in ^{190,192}Os.

The overall level spectra fits (table 3) are satisfactory and the E2 predictions (table 4) are seen to be in good agreement

with experiment. In particular, (i) the cross over/step over γ-ray decay ratio of the 2_2^+ level [$B(E2;2_2^+\rightarrow 0_1^+)/B(E2;2_2^+\rightarrow 2_1^+)$] is well reproduced, and (ii) the quadrupole moments of the 2_1^+ and 2_2^+ levels are predicted to be approximately equal in magnitude and opposite in sign in each nuclide in accord with experiment.

In the strict O(6) limit with $\beta \ll \alpha$ (i.e. $\beta=0$), the $B(E2;2_2^+\rightarrow 0_1^+)$ vanishes as well as do the quadrupole moments. Therefore, the degree of symmetry breaking required to fit the energy level spectra is seen also to be consistent with that needed to reproduce the E2 decays and quadrupole moments from and of, respectively, the 2^+ levels in ^{190,192}Os.

The predicted g-factor corrections, g_c, may be obtained for the levels of interest in these two nuclides using the calculated wave functions and the measured multipolarity mixing ratios for the $2_2^+ \rightarrow 2_1^+$ transition decays in ^{190}Os ($|\delta|=4.8\pm0.6$) (ref.22) and ^{192}Os ($|\delta|=8.5\pm2.5$) (ref.15) as prescribed.[2,3] We find that g_c = 0.014 and 0.020, respectively, for ^{190}Os and ^{192}Os.

Using[2]

$$g(L) = g \pm g_c\left(\frac{1}{10}\right)\left[\frac{(2L-1)(2L+3)}{L(L+1)(2L+1)}\right]^{\frac{1}{2}}\langle \alpha L||(d^+s)^2+(s^+d)^2||\alpha L\rangle \ , \qquad (10)$$

we find $|g(2_2^+)-g(2_1^+)|$ to be 0.024 (^{190}Os) and 0.028 (^{192}Os) with $g(4_1^+)=g(2_1^+)$ in both nuclides. Although the corresponding

differences in the gyromagnetic ratios for the 2_2^+ and 2_1^+ states in ^{196,198}Pt were not inconsistent with our experimental determinations[2,3], the differences predicted here for ^{190,192}Cs are at variance with the present measurements (table 2).

In assessing the disparity between these IBA-based predicted g-factor variations and the experimental values, it should be noted that for a given multipolarity mixing ratio, δ, in an $L \to L$ transition in a particular nuclide, the difference (Δg) between the calculated $g(2_2^+)$ and $g(2_1^+)$ values scales essentially as

$$\Delta g \approx \frac{\langle \alpha L || [(s^\dagger d)^2 + (d^\dagger s)]^2 || \alpha L \rangle}{\delta \langle 2_1^+ || [(s^\dagger d)^2 + (d^\dagger s)^2] || 2_2^+ \rangle} \qquad (11)$$

and, hence, is determined by the relative magnitudes of the structure matrix elements. For nuclei at the O(6) limit, the numerator in eq.(11) vanishes and the denominator is large, leading to g-factor constancy ($\Delta g \to 0$). However, for broken symmetry, if the system tends from O(6) toward SU(3) symmetry, the nuclear structure factor becomes more favourable and will be large in the SU(3) limit. (That this is the case can be essentially seen by taking the 2_2^+ level as the K=2 member of the γ-band [$(\lambda,\mu) \equiv (2N-4,2)$] representation and the 2_1^+ state as the ground-band (2N,0) representation in the N-boson SU(3) limit.[20] In this symmetry $Q(2_2^+)/Q(2_1^+) = -(4N-3)/(4N+3) \approx -1$ (N=8 for ^{192}Cs), in agreement with experiment; the numerator of eq.(11) - scaling as the in-band quadrupole matrix element - is large, whereas its denominator (scaling as the cross-over band matrix element) is relatively small, leading to a departure of Δg from zero.)

We stress that the interaction Hamiltonian [eq.(8)] does not provide a particularly sensitive test of the calculated-experimental g-factor comparisons, in that the χ^2 minimum of the least-squares fits to the energy level spectra are quite flat. For example, a feasible alternative set of parameters (at least insofar as the energy level spectra are concerned) is [A,B,C,D = -0.311, -0.618, 0.0049, 0.0312]; this set is much closer to the SU(3) limit than is the parameter fit set of table 3 and yields $|g(2_1^+)-g(2_2^+)| = 0.067$ (^{192}Os) and 0.037 (^{190}Os), still smaller than, but in better agreement with, the experimental value $\Delta g = 0.115 \pm 0.028$ for ^{192}Os. Nevertheless, this more SU(3)-prone parameter set, while still reasonably well reproducing the static quadrupole moments in these nuclides, yields much smaller values for the calculated $B(E2;2_2^+ \rightarrow 2_1^+)$ rates in both ^{190}Os (461 e^2fm^4) and ^{192}Os (157 e^2fm^4) which are in strong disagreement with experiment.

In light of the foregoing and referring back to eq.(10) as a guide, it is not possible to simultaneously explain both the B(E2) data and experimental g-factor variation in terms of this IBA-based model. While conventional wisdom[1,8] holds that the Os-Pt region is well described by a perturbed O(6) boson model, we conclude that the measured g-factor variation cannot be encompassed in terms of the boson perturbation expansion, eq.(8).

As magnetic transitions and static moments are much more sensitive to single particle transitions (orbitals) than are

B(E2)s {g(single-particle) $\gtrsim$ g(collective) = Z/A}, it proves instructive to now consider a simple single-particle model.

5.3 Single-particle model calculations

In the work of Götz et al.[23], potential energy surfaces were given for the transition region and it was suggested that the Os isotopes (^{192}Os in particular) could be considered as nuclei with competing prolate and oblate axially symmetric shapes (γ=0,60°,respectively); an idea which has been useful in treating quadrupole and dipole moment systematics in (sd)-shell nuclei.[24]

To test the sensitivity of the $g(2_1^+)$ to such shape variations, the M1 dipole matrix element is calculated in the projected Hartree-Fock (PHF) formalism using a single determinant of deformed single-particle orbitals[25]

$$|\alpha LM\rangle = P^J_{MK}|\psi_K\rangle|\langle\psi_K|P^J_{KK}|\psi_K\rangle \ , \qquad (12)$$

$$\langle\alpha L||T(M1)||\alpha L\rangle = \frac{1}{\sqrt{3}} \sum_{j_1 j_2} S^{LL}_{j_1 j_2} M^{\prime}_{j_2 j_1}$$

where $S^{LL}_{j_1 j_2} = \langle\alpha L||(a^{\dagger}_{j_2} \otimes \tilde{a}_{j_1})^1||\alpha L\rangle$ is the reduced single particle density matrix and $M^{\prime}_{j_2 j_1}$ is the single particle reduced matrix element. In the evaluation of M, we set g^{ℓ}_p=1,g^{ℓ}_n=0 and quench the spin g-factors (g^s_p=5.586;g^s_n= -3.826) by 0.6 (which is usual in this mass region[26]).

The determinant $|\psi_K>$ was constructed using the Nilsson levels of Irvine[27]

$$|\psi_K> = \prod_{\alpha=1}^{A} b_\alpha^\dagger |-> , \qquad (13)$$

where $|->$ is the ^{208}Pb core and the $b_\alpha^\dagger$ are the one-hole creation operators. The single-particle basis is the N=4 shell + $0h_{11/2}$ for protons and the N=5 shell + $0i_{13/2}$ shell for neutrons. This Nilsson basis is consistent with the level scheme of Götz et al.[25] near ^{184}W. Ground-state bands are assumed to be the pair-wise filled time-reversal symmetric state with K=0, and excited states appear from shape mixing (oblate-prolate) or particle-hole excitation. Although we cannot obtain collective shape asymmetry ($\gamma \neq 0$) with axially symmetric single-particle levels, yet the sensitivity of g(L) to single-particle excitations can be tested. The results of such a test are shown for ^{192}Os in table 5 where it can be seen that (i) the PHF determinant can reasonably well reproduce the measured absolute $g(2_1^+)$ for prolate shapes that are consistent with $Q(2_1^+)$, with g being relatively insensitive to the shape parameter, δ, for $\delta \geq 0.1$, and (ii) small oblate shapes have a small (perhaps negative) g-factor inconsistent with any of the gyromagnetic ratios measured for the 2_1^+, 2_2^+, and 4_1^+ states.

For a prolate shape of $\delta = 0.2$, the lowest 2p-2h K=0 excitation has a $g(2^+)$ value of +0.144, while the lowest K≠0 1p-1h excitation has $g(2^+) = 0.812$ (proton excitation) and $g(2^+) = -0.519$ (neutron excitation).

It appears clear that, due to the lack of quenching in the non-time-reversal symmetric states, the g-factors calculated in this model are sensitive to K≠0 admixtures; but equally, the variation in the g-factors of the K=0 excited bands could encompass the scale of variations observed experimentally in the Os isotopes. Calculations of $g(2_1^+)$ for the lighter even Os isotopes for $0.1 < \delta < 0.3$ range from 0.2 to 0.3, again in rough agreement with experiment (see table 2).

We conclude that the simple model, above, based on a single axially symmetric Nilsson Slater determinant indicates that a study of g-factors, B(E2)s, and $Q(2^+)$ variations in the Os isotopes using a more detailed microscopic model would be useful. As an interim step, the semi-phenomenological Bose-Fermi models,[28] which have been successful in the high-spin Pt levels, may be able to reproduce large g-factor variations.

6. Conclusions.

The extensive body of empirical information, comprised of the present measurements of the gyromagnetic ratios of the 2_1^+, 2_2^+ and 4_1^+ states in ^{192}Os, available prior g-factors measured for corresponding levels in ^{190}Os, relevant B(E2) rates, and the measured quadrupole moments of the 2_1^+ and 2_2^+ states in both nuclides, has been compared with predictions calculated on symmetry-broken O(6) IBA bases and on deformed single-particle model considerations.

Although these models have been shown capable of accommodating some measure of g-factor variations for the levels of interest, neither one appears able to predict simultaneously both the experimentally observed gyromagnetic ratios and B(E2) transition rates adequately well. These findings suggest that some degree of both collective and particle-orbital effects are required to encompass the dynamic and static moment data now available for these transitional nuclei.

The authors appreciate most sincerely the cooperation and hospitality provided by the staff of the Australian National University 14 UD Pelletron laboratory, the aid provided by Professors H. Ohnuma and G.B. Beard in experimental facets of this investigation, and informative consultations with Dr. A.A. Humffray on aspects of electroplating Os. One of us (C.G.R.) acknowledges the assistance of a Commonwealth Post-Graduate Research Award. This research was supported, in part, by grants from the Australian Research Grants Scheme and Budget Rent-a-Car (Australia).

References

1. H.H. Bolotin, A.E. Stuchbery, I. Morrison, D.L. Kennedy, C.G. Ryan, and S.H. Sie, Nucl.Phys. A370 (1981) 146.
2. A.E. Stuchbery, C.G. Ryan, H.H. Bolotin, I. Morrison, and S.H. Sie, Nucl.Phys. A365 (1981) 317.
3. A.E. Stuchbery, C.G. Ryan, I. Morrison, and H.H. Bolotin, Phys.Rev.C 24 (1981) 2106.
4. F. Iachello and A. Arima, Phys.Lett. 53B (1974) 309.
5. A. Arima and F. Iachello, Phys.Rev.Lett. 35 (1975) 1069.
6. A. Arima and F. Iachello, Ann.Phys. (N.Y.) 99 (1976) 253.
7. A. Arima and F. Iachello, Phys.Rev.Lett. 40 (1978) 385.
8. R.F. Casten and J.A. Cizewski, Nucl.Phys. A309 (1978) 477; R.F. Casten and J.A. Cizewski, Phys.Lett. 79B (1978) 5; R.F. Casten, M.R. MacPhail, W.R. Kane, D. Breitig, K. Schreckenbach, and J.A. Cizewski, Nucl.Phys. A316 (1979) 61..
9. A.E. Stuchbery, C.G. Ryan, H. Ohnuma, G.B. Beard, and H.H. Bolotin, Phys.Rev.C (in press); A.E. Stuchbery, C.G. Ryan, and H.H. Bolotin, Hyp.Int. (in press).
10. G. Van Middlekoop, Hyp.Int. 4 (1978) 238; N. Benczer-Koller, M. Hass, and J. Sak, in Annual Review of Nuclear and Particle Science, eds. J.D. Jackson, H.E. Gove, and R.F. Schwitters (Annual Reviews, Inc., Palo Alto, 1980) Vol. 30, p.53; and references cited in these review papers.
11. A.E. Stuchbery, C.G. Ryan, and H.H. Bolotin, Phys.Rev. C24 (1981) 1480.

12. A. Winther and J. de Boer, Coulomb Excitation, edited by K. Alder and A. Winther (Academic, New York, 1966), p.303.

13. A.E. Stuchbery, Ph.D. thesis, University of Melbourne, 1981 (unpublished).

14. H. Morinaga and T. Yamazaki, in In-Beam Gamma-Ray Spectroscopy (North-Holland, Amsterdam, 1976), chap.2.

15. M.R. Schmorak, Nucl.Data Sheets 9 (1973) 195.

16. J.F. Ziegler, Appl.Phys.Lett. 31 (1977) 544.

17. Table of Isotopes, 7th ed., edited by C.M. Lederer and V.S. Shirley (Wiley, New York, 1978), Appendix VII, in which previously reported measurements of the magnetic moments of the levels in the even Os nuclides are tabulated and referenced.

18. A.S. Davydov and G.F. Filipov, Nucl.Phys. 8 (1958) 237.

19. J.P. Davidson, Rev.Mod.Phys. 37 (1965) 105.

20. A. Arima and F. Iachello, Ann.Phys. (N.Y.) 111 (1978) 201.

21. M.R. Schmorak, Nucl.Data Sheets 9 (1973) 401.

22. C. Baktash, J.X. Saladin, J.J. O'Brien, and J.G. Alessi, Phys.Rev. C22 (1980) 2373.

23. U. Götz, H.C. Pauli, and K. Alder, Nucl.Phys. A192 (1972) 1.

24. I. Morrison, Phys.Lett. 91B (1980) 4.

25. G. Ripka, Advances in Nuclear Physics, ed. by M. Baranger and E. Vogt (Plenum Press, N.Y.), Vol. 1 (1968) 183.

26. A. Faessler, Proceedings of the Gull Lake Conference, Michigan, 1979, Lecture Notes in Physics (Springer-Verlag, Berlin, 1979).

27. J.M. Irvine, Nuclear Structure Theory (Pergamon Press, London, 1972).

28. I. Morrison, A. Faessler, and C. Lima, Nucl.Phys. A372 (1981) 13.

Table 1. Present experimental particulars and results for ^{192}Os recoiling through a 4.2 μm thick magnetized Co foil.

Level	Mean life τ (psec)	T_{Co}[a] (fs)	E_i[a] (MeV)	E_o[a] (MeV)	$(v/v_o)_i$[a]	$(v/v_o)_o$[a]	$\langle v/v_o \rangle$[a]	ε(65°)[b] (×10³)	S(25°)[c]	R(mrad)[d]	Δθ (mrad)	Experimental g factors: Present Work[f]	Prior Work[g]
2_1^+	418	522	136	28	5.3	2.4	3.7	42.6(14)	-1.62(5)	-1.57(5)	-26.4(12)[e]		0.365(10)
2_2^+	46	522	136	28	5.3	2.4	3.7	44.4(42)	-2.46(7)	-2.46(7)	-18.0(18)	0.250(26)	0.28 (10)
4_1^+	20	522	136	28	5.3	2.4	3.7	26.1(28)	-0.99(3)	-0.99(3)	-26.4(29)	0.365(45)	

[a] Transit time of recoiling Os ions through Co foil, energies of the ions incident upon, E_i, and emergent from, E_o, the Co foil, velocities of these ions relative to that of the Bohr velocity, $v_o = c/137$, entering, $(v/v_o)_i$, and leaving, $(v/v_o)_o$, the Co foil, and the average velocity of the ions, $\langle v/v_o \rangle$, in the foil were obtained using the known target and Co foil thicknesses, the known reaction kinematics, and the stopping powers of ref. 14.

[b] The experimental ratio $\varepsilon = (1-\rho)/(1+\rho)$ multiplied by 10^3, where $\rho = \{[N\uparrow(+)N\uparrow(-)]/[N\uparrow(+)N\uparrow(-)]\}^{\frac{1}{2}}$ measured with two detectors positioned at (±) the specified angle, and N↑(N↓) are normalized counting rates recorded for polarizing field up(down).

[c] The values of S [logarithmic derivative of W(θ)] for the transitions at the designated angle were calculated and measured for the present experimental geometry (see text).

[d] See definition of R, eq.(2), text.

[e] Corrected for small precession of ^{192}Os 2_1^+ state (τ = 418 psec) in external polarizing field.

[f] The g factors obtained in the present work are relative to the weighted average of previous determinations of the gyromagnetic ratio of the 2_1^+ level in ^{192}Os (presented in the last column).

[g] Weighted averages of prior values reported in the literature for the states of interest (summary of previous measured values are presented in Ref. 17).

Table 2. Summary of experimentally determined gyromagnetic ratios reported for the designated levels in the even $^{186-192}$Os nuclides.

Level (J^π;isotope)	Experimental gyromagnetic ratio	$g(2_2^+)/g(2_1^+)$	$g(4_1^+)/g(2_1^+)$
$2_1^+;^{186}$Os	0.282 ± 0.007[a]		
$2_1^+;^{188}$Os	0.294 ± 0.008[a]	1.54 ± 0.26	
$2_2^+;^{188}$Os	0.453 ± 0.074[a]		
$2_1^+;^{190}$Os	0.297 ± 0.009[a]		≈1.5
$4_1^+;^{190}$Os	≈0.45[a]		
$2_1^+;^{192}$Os	0.365 ± 0.010[a]	0.68 ± 0.08[b]	1.00 ± 0.12[b]
$2_2^+;^{192}$Os	0.250 ± 0.026[b]		
$4_1^+;^{192}$Os	0.365 ± 0.045[b]		

[a] Weighted average of prior determinations presented in Ref. 17.

[b] Present results; measured relative to $g(2_1^+;^{192}$Os).

Table 3. Least-squares fit boson Hamiltonian parameters and calculated and experimental level spectra of ^{190,192}Os.

	^{190}Os	^{192}Os
Parameters[a]		
A	123	147
B	157	167
C[b]	-0.76	-0.55
D	11	12
J^π	Energy levels (keV) Experiment [calculated]	Energy levels (keV) Experiment [calculated]
2_1^+	187 [162]	206 [180]
2_2^+	558 [589]	439 [486]
4_1^+	548 [505]	580 [538]
3_1^+	756 [837]	690 [777]
4_2^+	955 [996]	910 [909]
6_1^+	1050[1016]	1089[1063]
0_2^+	912 [808]	[677]
2_3^+	1115[1144]	[1049]
4_3^+	1163[1326]	[1222]

a) Parameter values are in keV.

b) It should be noted that the values of the parameter C found by Casten et al. (ref. 8) are approximately 8 times larger than obtained in the present fits due to differences in the definition used for the quadrupole operator.

Table 4. Comparison of present calculated B(E2) transition rates[a] and static quadrupole moments with experimental values from and of the 2_1^+ and 2_2^+ states in ^{190,192}Os.

	^{190}Os	^{192}Os
	Experiment [calculated]	Experiment [calculated]
$B(E2;2_1^+\rightarrow 0_1^+)e^2fm^4$	4760 ± 120[b] [5142]	4080 ± 120[c] [4390]
$B(E2;2_2^+\rightarrow 0_1^+)e^2fm^4$	460 ± 24[b] [587]	402 ± 20[c] [417]
$B(E2;2_2^+\rightarrow 2_1^+)e^2fm^4$	2600 ± 150[b] [2782]	3600 ± 300[c] [2915]
$Q(2_1^+)$ efm^2	-80 ± 30[d] [-125]	-70 ± 30[d] [-97]
$Q(2_2^+)$ efm^2	+90 ± 40[d] [+127]	+80 ± 30[d] [+99]

a) Calculated using $(\alpha,\beta) = (16.1,1.5)$, see text eq.(9).

b) Ref. 21.

c) Ref. 15.

d) Ref. 22.

Table 5. Gyromagnetic ratio values in ^{192}Os calculated using Irvine[a] levels for a range of shape parameter, δ, values taking $\mu = 0.625$ and $K = 0.050$.

δ	-0.3	-0.2	-0.1	0	0.1	0.2	0.3
$\lvert\psi_{g.s.}\rangle g(2_1^+)$	0.167	0.116	-0.027	[b]	0.283	0.295	0.307

a) Ref. 27.

b) The g-factor value for a spherical (δ=0) nucleus depends upon the partially filled shell (presumed neutrons); for the $(d_{3/2})^{-2}$ configuration $g(2_1^+) = -0.765$, and for the $(d_{5/2})^{-2}$ configuration $g(2_1^+) = 0.328$.

Figure captions.

Figure 1: Relevant portion of the spectrum of de-excitation γ rays detected at 65° to the beam direction in coincidence with backscattered projectiles following Coulomb excitation of the composite ^{192}Os-^{198}Pt target by 220-MeV ^{58}Ni ions. Transitions are labelled by $J_i^\pi \rightarrow J_f^\pi$ and isotope. Small, but discernible on this semi-log plot, are attenuated Doppler-shift shoulders on the high-energy sides of transitions from relatively short-lived states which decay as the Os and Pt ions slow before coming to rest in the Pb target backing. Chance coincidences have been subtracted.

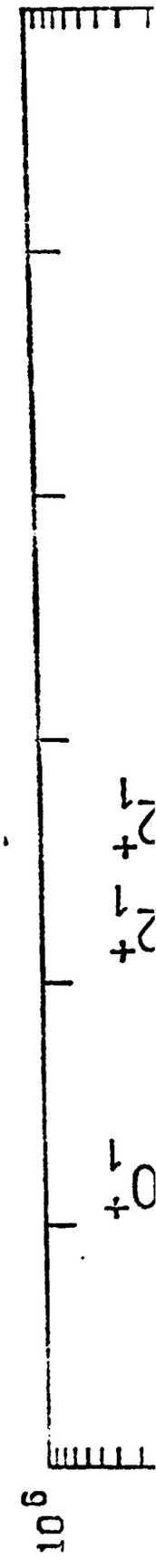

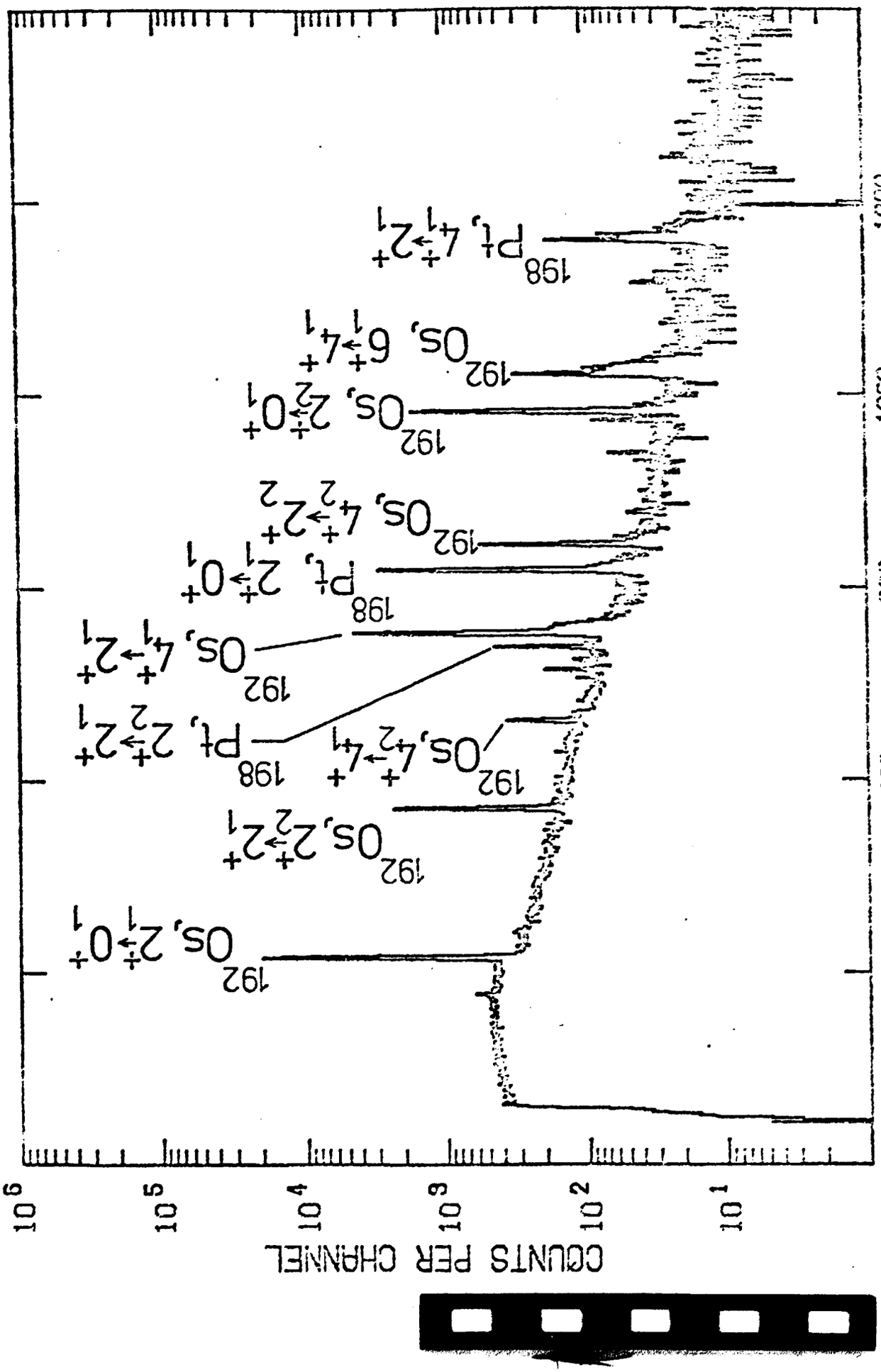
COUNTS PER CHANNEL
10^6
10^5
10^4
10^3
10^2
10^1
400
600
800
1000
1200
CHANNEL NUMBER
^{192}Os, $2_1^+ \rightarrow 0_1^+$
^{192}Os, $2_2^+ \rightarrow 2_1^+$
^{192}Os, $4_2^+ \rightarrow 4_1^+$
^{198}Pt, $2_2^+ \rightarrow 2_1^+$
^{192}Os, $4_1^+ \rightarrow 2_1^+$
^{198}Pt, $2_1^+ \rightarrow 0_1^+$
^{192}Os, $4_2^+ \rightarrow 2_2^+$
^{192}Os, $2_2^+ \rightarrow 0_1^+$
^{192}Os, $6_1^+ \rightarrow 4_1^+$
^{198}Pt, $4_1^+ \rightarrow 2_1^+$

Figure 1.